5th International Symposium on Three-Dimensional Electromagnetics
Sapporo, Japan, May 7–9, 2013

Convergence studies for the finite element simulation of the 3D MT boundary value problem

Antje Franke-Börner, Ralph-Uwe Börner, and Klaus Spitzer
TU Bergakademie Freiberg, Germany

SUMMARY

We present convergence studies for the three-dimensional magnetotelluric boundary value problem. The equation of induction is solved with the help of the finite element method in a bounded domain Ω applying Dirichlet and Neumann boundary conditions. For the model of a homogeneous halfspace, the error of the numerical solution with respect to the analytical solution is considered for a hierarchy of nested unstructured tetrahedral meshes. We examine the convergence behaviour with increasing number of degrees of freedom in dependence of the order p of the finite elements (p = 1, 2, 3), the frequency f of the electromagnetic fields (f = 0.01, 0.1, 1 Hz), and the mesh refinement strategy applied. If the true solution is unknown, convergence studies are performed using the numerical finest-grid solution for comparison. These studies are subsequently used to evaluate the quality of different formulations of the three-dimensional magnetotelluric boundary value problem that arise from Maxwell's equations. Exemplarily, the equation of induction is derived in terms of the magnetic field, the electric field, the magnetic vector potential and the electric scalar potential as well as the anomalous magnetic vector potential. Our computations illustrate that the convergence behaviour varies with the conductivity distribution in the model. Furthermore, global convergence results do not necessarily apply to local convergence, e. g., at arbitrary data points on the earth's surface. We finally demonstrate the merit of convergence studies for the estimation of the accuracy of the numerical solution for a close-to-reality model of Stromboli volcano.

Keywords: magnetotellurics, finite element method, boundary value problem, 3D, numerical simulation

INTRODUCTION

The quality of a numerical simulation approach is mainly determined by the accuracy of the solution and the computational cost, i. e., memory requirements and run time. The finite element (FE) formulations of different three-dimensional (3D) magnetotelluric (MT) boundary value problems arising from Maxwell's equations are examined under these aspects in terms of convergence studies. Using several steps of uniform or adaptive mesh refinement (h-refinement) and increasing the polynomial degree of the basis functions (p-refinement) up to $p = 3$ the convergence of the FE solution for a homogeneous halfspace model towards the analytical solution is demonstrated for the frequencies $f = 0.01, 0.1, 1\,\mathrm{Hz}$ to verify expectations according to convergence theory. In general, for 3D conductivity structures the true solution is unavailable, hence, the convergence of the numerical result to the finest-grid solution is analysed. These convergence studies illustrate that even simple conductivity structures affect the convergence behaviour which is mainly dependent on the regularity of the true solution. We consider formulations of the MT boundary value problem (BVP) derived in terms of the magnetic field $\mathbf{H}$ and the electric field $\mathbf{E}$ in order to examine if the convergence rate reflects the different behaviour of $\mathbf{H}$ and $\mathbf{E}$ with regard to continuity at conductivity jumps. Using the formulation of the MT BVP in terms of the magnetic vector potential $\mathbf{A}$ and the electric scalar potential ϕ we augment the curl-curl equation of induction with the equation of continuity and investigate the influence of this stabilization on the convergence behaviour of the numerical solution. Furthermore, formulating the BVP in terms of the anomalous magnetic vector potential enables the numerical solution of the linear system of equations in the absence of the normal electromagnetic fields which are orders of magnitude larger than the anomalous fields.

THE 3D BOUNDARY VALUE PROBLEMS

Based on Maxwell's equations and assuming a harmonic time dependency $e^{i\omega t}$ with frequency f, angular frequency $\omega = 2\pi f$ and the imaginary unit i, the 3D MT BVP in the domain Ω can be formulated in terms of the magnetic field $\mathbf{H}$ (BVP 1)

$$\begin{aligned}
\nabla\times(\sigma+i\omega\varepsilon)^{-1}\nabla\times\mathbf{H}+i\omega\mu\mathbf{H} &= 0 \quad \text{in} \quad \Omega\\
\Gamma_{\perp}: \quad \mathbf{n}\times\mathbf{E} &= 0\\
\Gamma_{||}: \quad \mathbf{n}\times\mathbf{H} &= 0\\
\Gamma_{\text{top}}\cup\Gamma_{\text{bot}}: \quad \mathbf{H} &= \mathbf{H}_n(x,y,z)\\
\Gamma_{\text{int}}: \quad \mathbf{n}_1\times\mathbf{E}_1-\mathbf{n}_2\times\mathbf{E}_2 &= 0, \qquad (1)
\end{aligned}$$

for electrical conductivity σ, magnetic permeability μ, dielectric permittivity ε, and normal unit vectors $\mathbf{n}$ where $\Gamma_\perp$ denotes all boundaries oriented perpendicularly to the horizontal current flow, $\Gamma_{||}$ includes all boundaries parallel to the horizontal current flow, Γ_{top} and Γ_{bot} are the horizontal top and bottom boundaries, respectively. For all exterior boundaries a 1D layered-halfspace model is assumed for which the magnetic field $\mathbf{H}_n$ can be calculated analytically (Wait, 1953). On all the interior boundaries Γ_{int}, representing possible jumps in the electromagnetic model parameters, the conditions of continuity of the tangential field components apply. Furthermore, for the electric field $\mathbf{E} = (\sigma + i\omega\epsilon)^{-1}\nabla \times \mathbf{H}$ is valid.

The BVP for the electric field $\mathbf{E}$ (BVP 2) reads

$$\begin{aligned} \nabla \times \mu^{-1}\nabla \times \mathbf{E} + (i\omega\sigma - \omega^2\varepsilon)\mathbf{E} &= 0 \quad \text{in} \quad \Omega \\ \Gamma_\perp : \quad \mathbf{n} \times \mathbf{E} &= 0 \\ \Gamma_{||} : \quad \mathbf{n} \times \mathbf{H} &= 0 \\ \Gamma_{\text{top}} \cup \Gamma_{\text{bot}} : \quad \mathbf{H} &= \mathbf{H}_n(x,y,z) \\ \Gamma_{\text{int}} : \quad \mathbf{n}_1 \times \mathbf{H}_1 - \mathbf{n}_2 \times \mathbf{H}_2 &= 0 \end{aligned} \tag{2}$$

using the same notation as above. Here, $\mathbf{H} = (-i\omega\mu)^{-1}\nabla \times \mathbf{E}$ applies.

The divergence-free field $\mathbf{B}$ can be expressed as the curl of the vector potential $\mathbf{A}$: $\mathbf{B} = \nabla \times \mathbf{A}$. Since $\nabla \times (\mathbf{E} + i\omega\mathbf{A}) = 0$, we can introduce the scalar potential ϕ so that

$$\mathbf{E} = -\nabla\phi - i\omega\mathbf{A}. \tag{3}$$

Substituting the electric field in eq. (2) yields the equation of induction for the magnetic vector potential $\mathbf{A}$

$$\nabla\times \mu^{-1}\nabla\times \mathbf{A} + (i\omega\sigma - \omega^2\varepsilon)\mathbf{A} + (\sigma + i\omega\varepsilon)\nabla\phi = 0. \tag{4}$$

To solve for both unkowns $\mathbf{A}$ and ϕ the equation of continuity $\nabla\cdot(\nabla\times \mathbf{H}) = \nabla\cdot((\sigma + i\omega\varepsilon)\mathbf{E}) = 0$ needs to be applied additionally. Therewith, the BVP in terms of the magnetic vector potential $\mathbf{A}$ and the electric scalar potential ϕ (BVP 3) can be formulated

$$\begin{aligned} \nabla\times \mu^{-1}\nabla\times \mathbf{A} + (i\omega\sigma - \omega^2\varepsilon)\mathbf{A} + (\sigma + i\omega\varepsilon)\nabla\phi & \\ = 0 \quad \text{in} \quad \Omega & \\ -\nabla\cdot \big((i\omega\sigma - \omega^2\varepsilon)\mathbf{A}\big) + ((\sigma + i\omega\varepsilon)\nabla\phi) & \\ = 0 \quad \text{in} \quad \Omega & \\ \Gamma_{||} : \quad \mathbf{n} \times \mathbf{H} = 0,\ \mathbf{n}\cdot\mathbf{j} = 0 & \\ \Gamma_\perp : \quad \mathbf{n} \times \mathbf{A} = 0,\ \phi = \phi_0 & \\ \Gamma_{\text{top}} \cup \Gamma_{\text{bot}} : \quad \mathbf{H} = \mathbf{H}_n(x,y,z),\ \mathbf{n}\cdot\mathbf{j} = 0 & \\ \Gamma_{\text{int}} : \quad \mathbf{n}_1 \times \mathbf{H}_1 = \mathbf{n}_2 \times \mathbf{H}_2,\ \mathbf{n}_1\cdot\mathbf{j}_1 = \mathbf{n}_2\cdot\mathbf{j}_2 & \end{aligned} \tag{5}$$

where $\mathbf{j} = -\big((i\omega\sigma - \omega^2\varepsilon)\mathbf{A} + (\sigma + i\omega\varepsilon)\nabla\phi\big)$ is the current density incorporating conduction and displacement currents.

The separation of the electric and magnetic fields $\mathbf{E}$ and $\mathbf{H}$, respectively, into normal ($\mathbf{E}_n$, $\mathbf{H}_n$) and anomalous ($\mathbf{E}_a$, $\mathbf{H}_a$) contributions $\mathbf{E} = \mathbf{E}_a + \mathbf{E}_n$ and $\mathbf{H} = \mathbf{H}_a + \mathbf{H}_n$ where $\nabla\times \mathbf{E}_n = -i\omega\mu_n\mathbf{H}_n$ and $\nabla\times \mathbf{H}_n = (\sigma_n + i\omega\epsilon_n)\mathbf{E}_n$ with

$$\varepsilon = \varepsilon_n + \varepsilon_a, \quad \sigma = \sigma_n + \sigma_a, \quad \mu = \mu_n + \mu_a$$

and substituting $\mathbf{E}_a = -i\omega\mathbf{A}_a$ results in the formulation of the BVP in terms of the anomalous magnetic vector potential $\mathbf{A}_a$ (BVP 4)

$$\begin{aligned} \nabla \times \mu^{-1}(\nabla \times \mathbf{A}_a - \mu_a\mathbf{H}_n) \quad + & \quad (i\omega\sigma - \omega^2\varepsilon)\mathbf{A}_a \\ = & \quad (\sigma_a + i\omega\varepsilon_a)\mathbf{E}_n \quad \text{in}\ \Omega \\ \mathbf{n} \times \mathbf{A}_a \quad = & \quad 0 \quad \text{on} \quad \Gamma_{\text{D}} \\ \mathbf{n}_1 \times \mathbf{H}_{a,1} - \mathbf{n}_2 \times \mathbf{H}_{a,2} \quad = & \quad 0 \quad \text{on} \quad \Gamma_{\text{int}} \end{aligned} \tag{6}$$

where $\mathbf{H}_a = \mu^{-1}\nabla \times \mathbf{A}_a$.

For the BVPs described by eqs (1), (2), (5), and (6), the resulting system of equations reads

$$\begin{pmatrix} \mathbf{K}^1 & \mathbf{K}^2 \\ \mathbf{M}^1 & \mathbf{M}^2 \end{pmatrix} \begin{pmatrix} \mathbf{U} \\ \mathbf{F} \end{pmatrix} = \begin{pmatrix} \mathbf{L} \\ \mathbf{N} \end{pmatrix} \tag{7}$$

where $\mathbf{K}^1$ and $\mathbf{M}^1$ represent the curl-curl equation of induction whereas $\mathbf{K}^2$ and $\mathbf{M}^2$ characterize the equation of continuity and vanish for eqs (1), (2), and (6). $\mathbf{U}$ is the numerical solution for the vector fields $\mathbf{H}$, $\mathbf{E}$, $\mathbf{A}$ or $\mathbf{A}_a$, respectively, and $\mathbf{F}$ denotes the numerical solution for ϕ. $\mathbf{L}$ contains inhomogeneous Neumann boundary condtitions for BVP 2 and 3 or the normal electromagnetic field for BVP 4, $\mathbf{N} \equiv 0$.

Eq. 7 is assembled using COMSOL Multiphysics™ COMSOL (2006). The inhomogeneous Dirichlet boundary conditions are eliminated by subtracting them from the system of linear equations. The system of equations is solved applying the PARDISO library (Schenk & Gärtner, 2006).

Assuming the exact solution with regularity $\mathbf{u} \in H^k(\Omega)$ and $\mathbf{u}_h \in V_{N_p}$ being the FE solution, for a family of quasi-uniform meshes the error $||e_h||_{H(curl)}$ of the numerical solution can be estimated in terms of the $H(curl)$-norm by

$$\begin{aligned} ||e_h||_{H(curl)} &= ||\mathbf{u} - \mathbf{u}_h||_{L^2} + ||\nabla\times u - \nabla\times u_h||_{L^2} \\ &\le CN^\alpha \end{aligned} \tag{8}$$

where $||\cdot||_{L^2}$ denotes the L^2-norm and C is a constant that is dependent on the regularity of the exact solution, the polynomial degree p of the basis functions, the modelling domain Ω, and the triangulation but does not depend on the exact solution $\mathbf{u}$ itself and the number N of degrees of freedom (Babuška & Szabo, 1982). The exponent

$$\alpha = -d^{-1}\ \min\{k, p\} \tag{9}$$

with dimensionality $d = 3$ for the 3D case is called the asymptotic rate of convergence or simply convergence rate. Sufficient regularity of the exact solution provided, i. e., $k > p$, the convergence rate α is governed by the order of the finite elements. Theoretical values are $\alpha(p = 1) = -0.33$, $\alpha(p = 2) = -0.67$, and $\alpha(p = 3) = -1.00$. For further details on the finite element method and a-priori error estimates the reader is referred to, e. g., Babuška & Aziz (1972).

CONVERGENCE STUDIES

For now, we consider the model of a homogeneous halfspace with electrical conductivity $\sigma = 0.01\,\mathrm{Sm}^{-1}$ for BVPs 1, 2, and 3. Later, BVP 4 is considered additionally in case of the presence of 3D conductivity structures.

Using a few steps of uniform and adaptive mesh refinement (h-refinement) and increasing the polynomial degree of the basis functions (p-refinement) up to $p = 3$ the convergence of the FE solution to the analytical solution can be demonstrated for the frequencies $f = 0.01, 0.1, 1\,\mathrm{Hz}$.

Figure 1 displays convergence curves for BVP 1, BVP 2, and BVP 3 described by eqs (1), (2), and (5), respectively. Shown are results for $f = 0.1\,\mathrm{Hz}$. We further consider the quantity

$$\text{relative rms} = \frac{\sum_{i=1}^{N} |F_i^{\mathrm{h}} - F_i|^2}{\sum_{i=1}^{N} |F_i|^2} \qquad (10)$$

as the rms error between the numerical solution F_i^h and the analytical solution F_i, $i = 1 \dots N$, N number of degrees of freedom (DOF). In contrast to the $H(curl)$-norm (cf. eq. (8)), this error measure gives an estimate of the average relative error of the numerical solution per DOF, however, exhibits the expected convergence behaviour as well.

The convergence rates are similar for all three formulations of the BVP and according to our expectations from eq. (9) (cf. Table 1). Note, that for the homogeneous case the numerical solution $\mathbf{u}$ is associated with a horizontal magnetic field component of $\mathbf{H}$ for BVP 1, but a horizontal electric field component of $\mathbf{E}$ for BVP 2 and 3. Accordingly, its curl $\nabla\times\,\mathbf{u}$ is proportional to $\mathbf{E}$ for BVP 1 and to $\mathbf{H}$ for BVP 2 and 3, respectively.

With increasing polynomial degree p of the basis functions the convergence rate α increases as expected from eq. (9). Figure 2 and Table 1 illustrate this behaviour.

Table 1. Convergence rate α for the numerical solution $\mathbf{u}$ and its curl $\nabla\times\,\mathbf{u}$ for BVP 1 - 3 for linear finite elements and for BVP 3 for linear, quadratic, and cubic finite alements.

$p = 1$, Figure 1			BVP 3, Figure 2		
bvp	$\alpha(\mathbf{u})$	$\alpha(\nabla\times\,\mathbf{u})$	p	$\alpha(\mathbf{u})$	$\alpha(\nabla\times\,\mathbf{u})$
1	-0.30	-0.43	1	-0.36	-0.41
2	-0.41	-0.36	2	-0.91	-0.62
3	-0.41	-0.36	3	-1.02	-0.82

CONCLUSION

We have carried out convergence studies that have confirmed the expected behaviour. For a homogeneous conductivity model we have obtained convergence rates for the numerical solution of BVP 1, 2 and 3 as predicted by convergence theory. Our numerical experiments have revealed that the convergence rates for the homogeneous models are independent of frequency and chosen uniform mesh refinement strategy. If jumps of electrical conductivity occur within the computational domain, the regularity of the exact solution is limited. Hence, the convergence rates are limited likewise.

Our numerical experiments further indicate that, in the case of the homogeneous model, there is no best choice of the BVP formulation. However, for models incorporating 3D conductivity structures, we expect BVP 4 to be superior to the other formulations. Moreover, it could be demonstrated that the analytical reference solution can be replaced by the numerical solution obtained for the finest grid without loss of significance.

REFERENCES

Babuška, I., & Aziz, A. K. (1972). *Survey lectures on the mathematical foundations of the finite element method with applications to partial differential equations* (A. K. Aziz, Ed.). Academic Press, New York.

Babuška, I., & Szabo, B. (1982). On the rates of convergence of the finite element method. *International Journal for Numerical Methods in Engineering*, *18*(3), 323–341.

COMSOL. (2006, August). COMSOL Multiphysics™ User's Guide, Version 3.5a [Computer software manual].

Schenk, O., & Gärtner, K. (2006). On fast factorization pivoting methods for symmetric indefinite systems. *Elec. Trans. Numer. Anal.*, *23*, 158-179.

Wait, J. R. (1953). Propagation of Radio Waves over a Stratified Ground. *Geophysics*, *20*, 416-422.

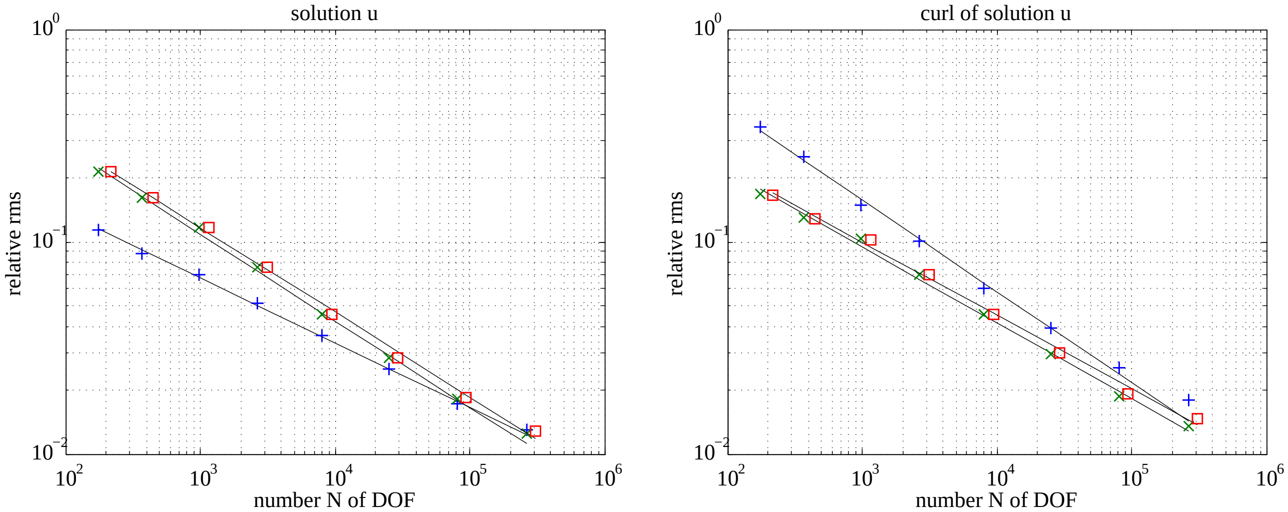

Figure 1. Convergence curves of the global relative rms error for the solution $\mathbf{u}$ (left-hand side) and its curl $\nabla\times\,\mathbf{u}$ (right-hand side) for BVP 1 (+), BVP 2 (×) and BVP 3 (□) at $f = 0.1$ Hz. Black lines (–) indicate the linear trend of each convergence curve .

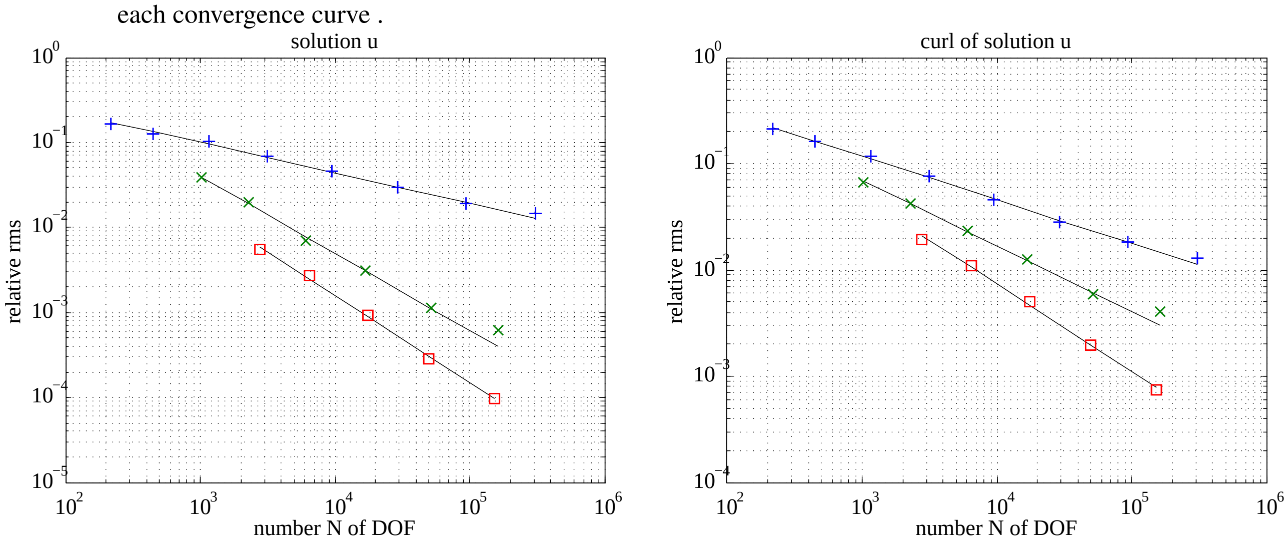

Figure 2. Convergence curves of the global relative rms error for the solution $\mathbf{u}$ (left-hand side) of BVP 3 and its curl $\nabla\times\,\mathbf{u}$ (right-hand side) using linear ($p = 1$, +), quadratic ($p = 2$, ×) and cubic ($p = 3$, □) finite elements at $f = 0.1$ Hz. Black lines (–) indicate the linear trend of each convergence curve.